RESEARCH ARTICLE   **Open Access**

A semi-passive beam dilution system for the FCC-ee collider

Alexander Krainer[1][*] , Wolfgang Bartmann[1], Marco Calviani[1], Yann Dutheil[1], Anton Lechner[1],
Antonio Perillo Marcone[1], Salim Ogur[1] and Rebecca Ramjiawan[1]

[*]Correspondence:
alexander.krainer@cern.ch
[1]CERN, Geneva, Switzerland

Abstract

The operation modes for the proposed FCC-ee collider foresee a very small beam spot size and stored beam energies of up to 20.6 MJ in Z production. This necessitates a dedicated beam dumping system. To reduce the complexity of the system as well as to minimize the required space, an optimized, semi-passive system has been designed and is presented here. The beam dilution is done with a defocusing triplet structure, followed by passive beam diluter elements (spoilers). This greatly reduces the risk of possible dilution failure scenarios compared to an active dilution kicker-magnet system. The dump core itself is located ∼70 m downstream of the spoilers and is designed following the experience gained from the LHC dump.

The dilution performance as well as the interaction effects responsible for the energy deposited in the spoiler, are directly related to the radiation length and the dimension of the device in beam direction. Materials for these spoilers have been studied extensively and key requirements have been identified using both Monte Carlo shower simulations and thermo-mechanical Finite Element Analysis. Even though the maximum temperature reached in the spoilers is well within the working temperature range of the material, the induced mechanical stresses can lead to material failure. Thermo-mechanical simulations have shown that the transversal beam shape plays a key role in the magnitude of mechanical stresses as a result of the beam impact and the abrupt temperature change. This problem is addressed in this paper and an optimized solution is presented.

1 Introduction

The Future Circular lepton Collider (FCC-ee) is a proposed ∼100 km, high luminosity, circular $e^+ e^-$ collider. If the circulating beam becomes unstable during collider operation, the beam parameters become unfavourable for physics or a system malfunction is detected within the collider systems, the first action is to remove the circulating beams from the ring. To ensure safe operation of the FCC-ee, beam disposal needs to be done in a safe and controlled way within one turn of the beam. The nominal operation foresees up to 3 to 4 such beam dumps per day, as outlined in the FCC-ee Conceptual Design Report [1].

Already in current (SuperKEKB [2]) and previous (LEP [3]) electron-positron colliders, it was necessary to dilute the beam in the transverse plane to ensure that the beam dump core material is not damaged. At SuperKEKB, with a stored beam energy of 0.18 MJ, this

Springer

Table 1 FCC-ee parameters for different operation modes [1]

	Z	WW	ZH	t$\bar{\text{t}}$	
Beam Energy [GeV]	45.6	80	120	175	182.5
Bunches / beam	16,640	2000	328	59	48
Bunch population [10^{11}]	1.7	1.5	1.8	2.2	2.3
Stored beam energy / beam [MJ]	20.6	3.84	1.13	0.36	0.32

dilution is done by introducing a ripple in the field of the extraction kickers and at LEP (stored beam energy of 0.12 MJ) dilution was achieved using passive beam diluters, so called spoilers, made from boron carbide.

As of today, the LHC beam dump system is the one capable of receiving the highest kinetic energy, corresponding to 539 MJ [4]. In this system, dilution is achieved by using dedicated pulsed dilution kicker magnets to create magnetic fields in two perpendicular planes, followed by ∼700 m of drift space before the dump block [5]. This ensures that every bunch of the extracted beam hits a different point on the beam dump. However, since additional active components are used to dilute the beam, a potential risk of dilution failure must be taken into account. The active components here are the dilution kicker magnets which are driven by a fast pulsed high voltage generators. For these components possible failure scenarios include for example, trigger signal failure of the kicker system or an electric failure in the voltage generators.

In the FCC-ee collider the highest stored beam energy will be 20.6 MJ for the Z operation mode (see Table 1). Having stored energies more than a factor 100 higher than all other electron-positron colliders, it becomes clear that a dedicated beam dumping system, based on a different technology than in other lepton colliders, is needed. To ensure high availability while also reducing the complexity of the system, a semi passive beam dumping system is introduced, using a defocusing triplet and spoilers for dilution.

2 Design of the FCC-ee extraction system

The extraction system is proposed to be located at the end of a Long Straight Section (LSS); a schematic of the extraction system is presented in Fig. 1. This configuration uses the arc of the collider ring after the LSS to increase the separation between the collider and dump, where this separation should be >5 m. The beam size at the spoiler should be σ_x > 11 mm horizontally and as large as possible vertically, to prevent damage to the spoiler. This is to be achieved with a defocusing quadrupole triplet in the extraction line. Beam parameters for the four FCC-ee energy modes are given in Table 2. The emittance is two orders of magnitude smaller vertically than the horizontally and consequently, the vertical β-value at the spoiler should be larger, with β_y > 1500 km.

With this scheme, a fast pulsed kicker would deflect the beam into the high-field region of a DC septum. A DC septum would help ensure the beam was dumped even in the event of a fast-time-scale failure. The kicker rise-time should be less than the abort gap, and to operate in the case of an asynchronous beam dump, the kicker flat-top should be long enough to cover the entire ring, i.e. >325 μs. To increase the deflection of the extracted bunch, the kicker and septum would, ideally, be placed at either side of a quadrupole, which is defocusing in the plane of extraction. Horizontal or vertical extraction is possible and the choice will depend on factors such as the booster-ring placement, the number of interaction points and the location of defocusing quadrupoles. For vertical extraction, a
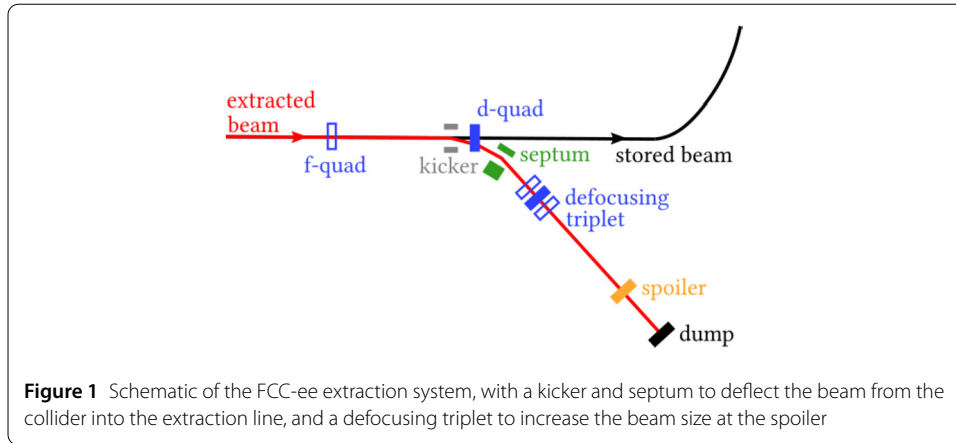
Figure 1 Schematic of the FCC-ee extraction system, with a kicker and septum to deflect the beam from the collider into the extraction line, and a defocusing triplet to increase the beam size at the spoiler

Table 2 FCC-ee beam parameters for four operation modes [1], where ϵ is the geometrical emittance, σ_δ is the energy spread and Bρ is the magnetic rigidity

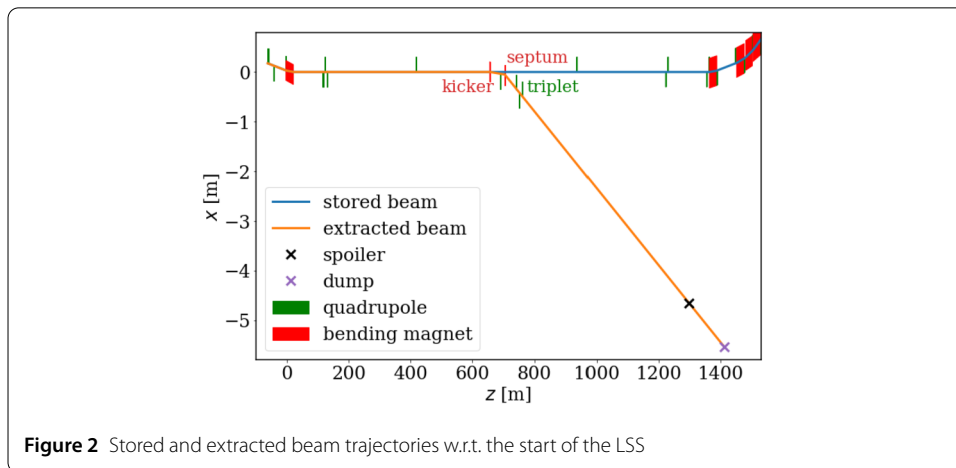| Parameter	Z	WW	ZH	$t\bar{t}$ (182.5 GeV)
ϵ_x/ϵ_y [nm, pm]	0.27/1.0	0.84/1.7	0.63/1.3	1.46/2.9
σ_δ (SR/BS) [%]	0.038/0.132	0.066/0.131	0.099/0.165	0.150/0.192
Bρ [Tm]	152.1	266.8	400.3	608.7

Figure 2 Stored and extracted beam trajectories w.r.t. the start of the LSS

kicker would extract the beam vertically and a defocusing magnet would magnify the deflection, a Lambertson septum would then horizontally deflect the beam. Here, the horizontal extraction is described (Fig. 2), considering Z-pole operation as this corresponds to the highest stored beam energy, 20.6 MJ (Table 1).

With this configuration, the spoiler and dump are located 680 m and 750 m downstream of the kicker, respectively. The kicker deflects the beam by 1 mrad and the septum by 6 mrad, producing a 5.1 m transverse separation of the beam dump from the beam axis. There is a 5.8 cm separation of the stored and extracted 5σ beam envelopes at the septum, so that a septum thickness of 4 cm would be suitable. The quadrupole triplet defocuses the beam to a 1σ spot size at the spoiler of 11.3 mm horizontally and 1.2 mm vertically (Fig. 3), corresponding to β_x = 200 km and β_y = 1500 km. The device parameters for the kicker, septum and quadrupoles for this configuration are given in Table 3. The kicker and the septum are within the limits of current technologies.
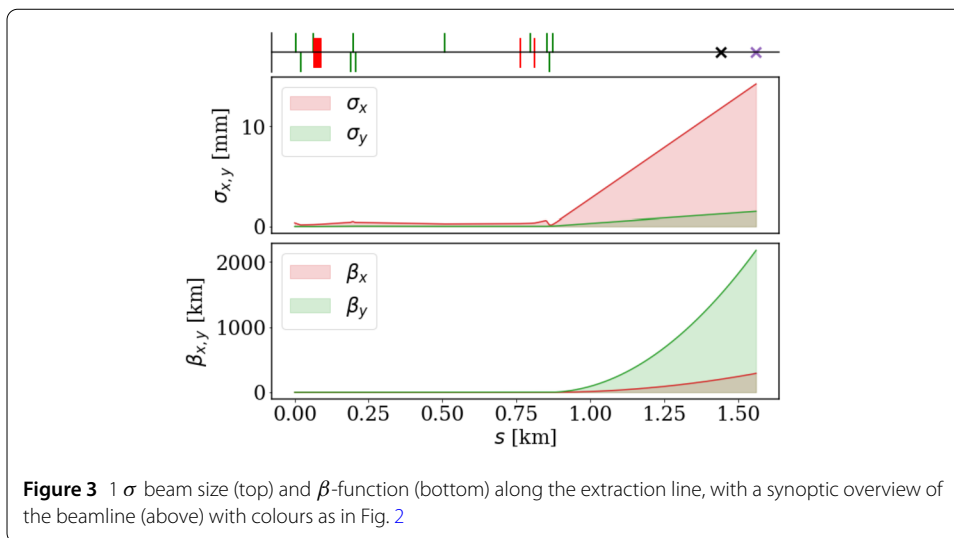
Figure 3 1σ beam size (top) and β-function (bottom) along the extraction line, with a synoptic overview of the beamline (above) with colours as in Fig. 2

Table 3 Device parameters for horizontal extraction from the collider ring. Parameters are for $t\bar{t}$-operation, as this is the most challenging in terms of magnet strengths. Quads 1–3 refer to the defocusing triplet

Magnet	Length	Field	1σ beam size (x, y)
Kicker	3 m	0.2 T	0.29, 0.023 mm
Septum	3 m	1.2 T	0.35, 0.023 mm
Quad 1	3 m	16.8 Tm^{-1}	0.50, 0.024 mm
Quad 2	3 m	-13.2 Tm^{-1}	0.14, 0.038 mm
Quad 3	3 m	16.8 Tm^{-1}	0.20, 0.036 mm

3 The semi-passive dilution system

When high-energy electrons or positrons impact on a material, they mainly lose energy by means of Bremsstrahlung processes in the Coulomb field of nuclei. On the other hand, the Bremsstrahlung photons generate electron-positron pairs, which in turn can produce further Bremsstrahlung photons. These processes lead to a particle multiplication, which is referred to as an electromagnetic shower. The repeated interactions in an electromagnetic shower can be described by means of the radiation length X_0, which represents a characteristic length both for Bremsstrahlung and pair production processes. For a carbon-based absorber material, the shower maximum is reached after about six radiation lengths at the lowest FCC-ee beam energy (45.6 GeV in Z operation mode), while it shifts to seven radiation lengths at the highest energy (182.5 GeV, $t\bar{t}$ operation mode).

The maximum energy deposition density and hence the peak temperature induced by the particle showers in a beam dump depend on the transverse beam size at the dump entrance. Due to the small size of the FCC-ee beams, a significant drift length is needed after the defocusing triplet quadrupoles in order to ensure the survival of the dump material. The peak load in the dump can be reduced by using a spoiler plate several tens of meters upstream of the dump, which acts as a passive beam diluter. The spoiler plate must be thin enough such that the shower build-up in the plate itself is limited, while it must be thick enough to enhance the angular spread of beam particles due to multiple Coulomb scattering. As discussed in the following, a good compromise between the two criteria is to limit the spoiler thickness to 0.1–0.2 radiation lengths. With such a spoiler, the total length of the dump line can be reduced by several hundred of meters.

3.1 Spoiler layout, materials and dilution performance

The Monte-Carlo particle transport code FLUKA [6–9] is used to simulate the energy deposited by the beam in the spoilers as well as in the beam dump. To reproduce the transversal beam distribution as closely as possible within FLUKA, a source routine is used to calculate the spot size as well as the beam spread and momentum dispersion directly from the optics functions and the beam emittance. This gives a transversal $1\,\sigma$ beam spot size at the spoiler of $\sigma_x \times \sigma_y = 1.1$ cm $\times$ 0.12 cm. The starting beam position is placed 5 cm upstream of the first spoiler. Three different spoiler configurations were simulated. A single 6 cm long spoiler as well as two 3 cm long spoilers spaced 5.5 m apart. To the latter configuration a third spoiler was added 3 m downstream. For all configurations the 4.3 m long beam dump is located 70 m downstream of the first spoiler. The length of the beam dump was chosen to correspond to about 13 X_0 for the graphite part ($X_{0\ (1.8\ \mathrm{g/cm^3})} =$ 23.72 cm, $X_{0\ (1.1\ \mathrm{g/cm^3})} = 38.82$ cm) and another $\sim$20 X_0 for the high density absorber at the end ($X_{0\ (8.9\ \mathrm{g/cm^3})} = 1.44$ cm). A sketch of the geometry is shown in Fig. 4.

The diameter for all spoilers was chosen to be 30 cm ($\sim$15 times the horizontal beam size) to accommodate steering errors and non-nominal beam dump scenarios. The spoiler core material was defined to be pure carbon with a density of 1.8 g/cm^3, which is an accurate molecular representation of isostatically pressed graphite as is foreseen for the FCC-ee spoilers (see below). The design of the beam dump core follows a similar approach as the current LHC dump, with a layered approach of high density and low density graphite blocks (see Fig. 4). The high density graphite at the beginning of the dump core produces a faster shower build-up and therefore reduces the overall dump length as compared to a complete low density core. This has almost no impact on the maximum energy deposition density within the core.

The material choice for the spoiler core is governed by the capability to withstand a high intensity beam impact without any permanent changes in the material structure. It therefore needs a high melting point as well as a large specific heat capacity and a low coefficient of thermal expansion over a wide temperature range. Furthermore, the mechanical properties as well as the availability and machinability of the material need to be considered. In existing beam-intercepting devices with similar requirements, carbon-based materials (such as isostatic graphite or carbon carbon composites) have been used successfully in
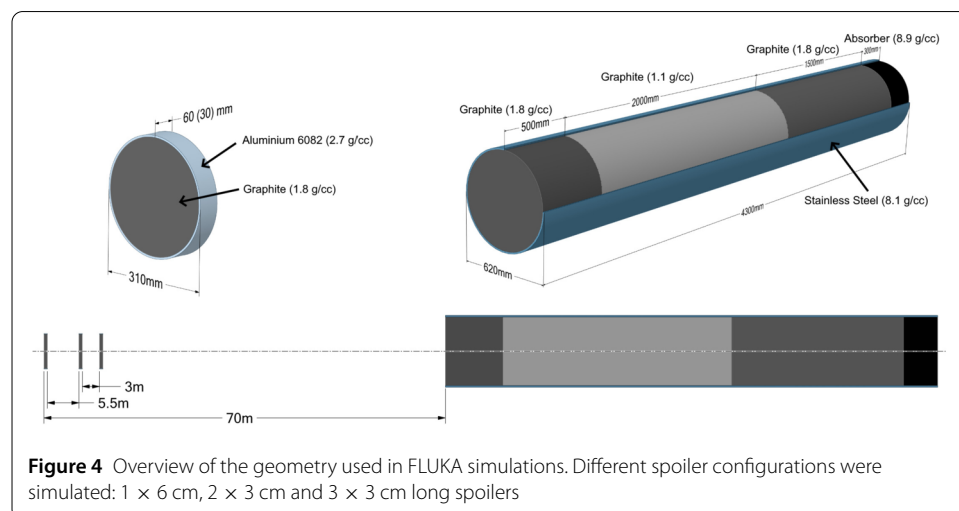

Figure 4 Overview of the geometry used in FLUKA simulations. Different spoiler configurations were simulated: 1 × 6 cm, 2 × 3 cm and 3 × 3 cm long spoilers

operation. Isostatic graphite has the advantage of being well characterized over a wide temperature range. This, as well as its isotropic nature, makes it possible to simulate it very accurately. Carbon-carbon composites on the other hand consist of carbon fibers inside a carbon matrix. By choosing the direction of these fibers, it is possible to increase the strength of the material in the plane where the highest stresses are expected. Due to this 3D structure with multiple layers and different properties on a microscopic and macroscopic scale it is much more complex to accurately simulate this type of material. As mentioned above, currently, isostatic graphite is foreseen for the spoiler core whereas the possible use of carbon-carbon composites is also under investigation.

3.2 Energy deposition in the spoiler

Figure 5 shows the longitudinal peak energy deposition in the spoiler core for the 6 cm and the 3 cm configurations assuming FCC-ee Z operation parameters (45.6 GeV, 16,640 bunches, 1.7×10^{11} particles/bunch). The expected maximum peak energy density on the spoiler is about 1.2 kJ/g for the 6 cm case and 0.95 kJ/g for the 3 cm spoilers. This corresponds to absolute adiabatic peak temperatures of 840°C (6 cm) and 720°C (3 cm) respectively. While these temperatures are well below the sublimation point of graphite, the temperature induced stresses on the downstream surface are not negligible. This is further increased by the extremely asymmetric beam shape which reflects in a very flat transversal energy deposition profile as can be seen in Fig. 6.

3.3 Energy deposition in the beam dump absorber

The beam dump core and vessel absorb approximately 96% of the full beam energy. Another 0.1% are absorbed in the spoilers. The remaining 3.9% are mostly absorbed in the shielding material surrounding the beam dump. In Fig. 7 the longitudinal peak energy density for the dump is shown. A peak energy density of 1.9 kJ/g (1200°C) is reached in the low density region of the beam dump in the configuration with three 3 cm spoilers. As can be seen, this is a factor 3 less peak energy density than without dilution. As mentioned before, the placement of high density graphite at the beginning of the dump core reduces
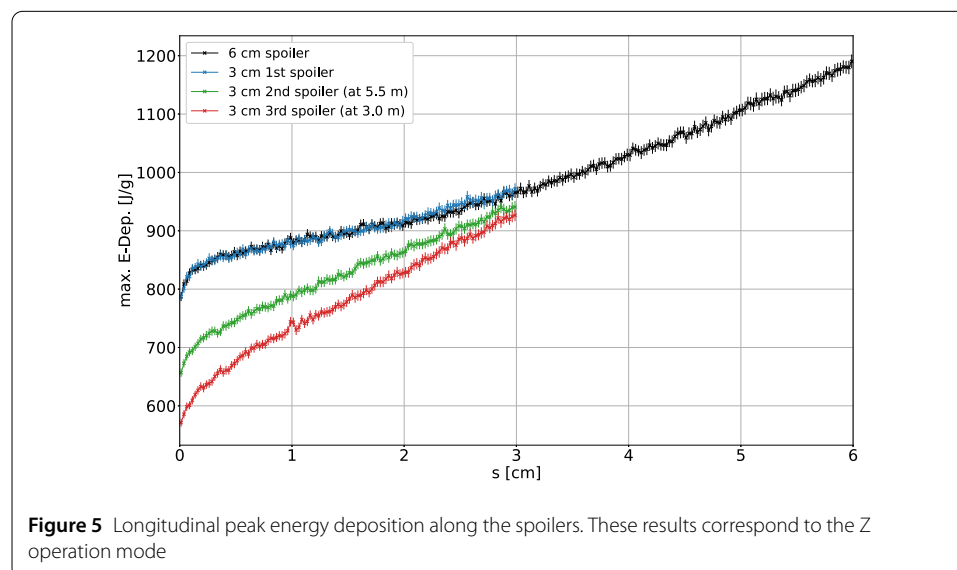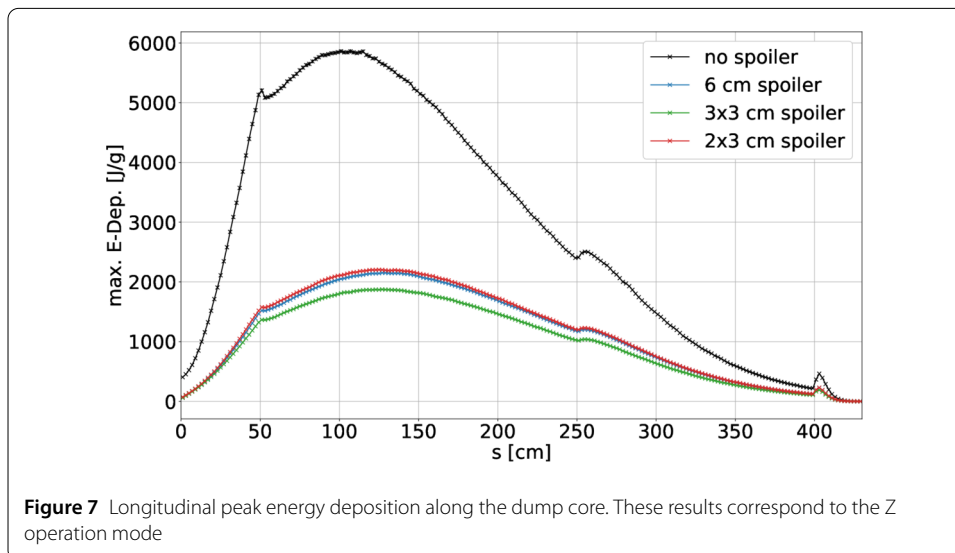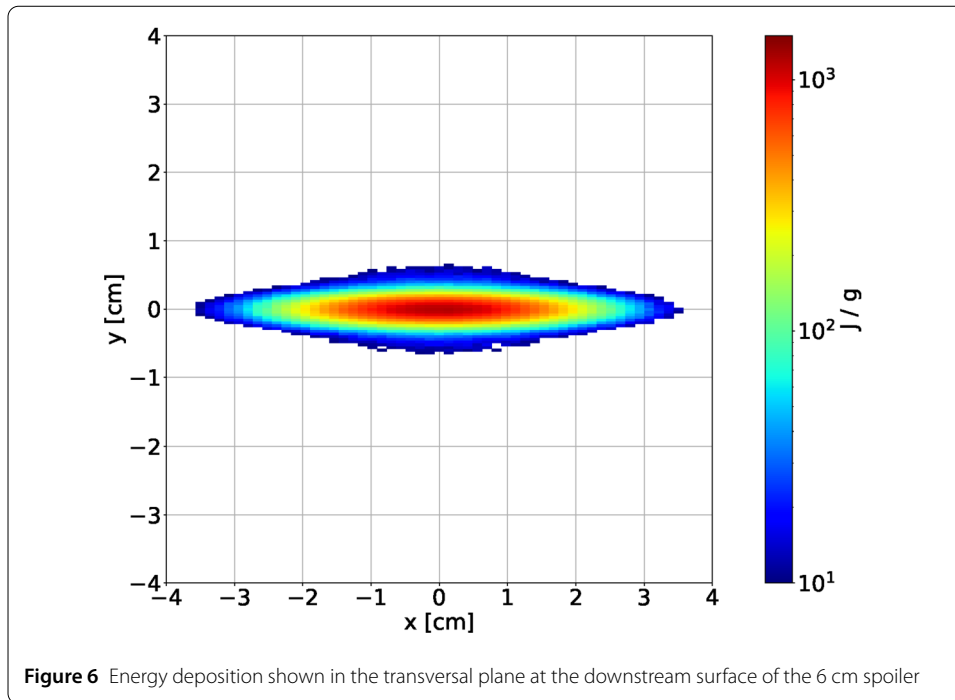

Figure 5 Longitudinal peak energy deposition along the spoilers. These results correspond to the Z operation mode

Figure 6 Energy deposition shown in the transversal plane at the downstream surface of the 6 cm spoiler

Figure 7 Longitudinal peak energy deposition along the dump core. These results correspond to the Z operation mode

the overall core length needed for absorbing the beam, without increasing the peak energy deposition or peak adiabatic temperature compared to a full low density dump. The 3x3 cm spoiler configuration produces similar maximum energy deposition values as expected for Run 3 of the LHC [4]. Since the dump material configuration is very similar to the LHC dump, it can be assumed that the proposed dump design would perform as required. The complete dump design will be a subject for detailed assessment in the future as it combines aspects from many different perspectives (i.e. radiation field around the dump, handling and remote access capabilities, instrumentation requirements).

Figure 8 Geometry and mesh used for LS-Dyna thermomechanical simulations
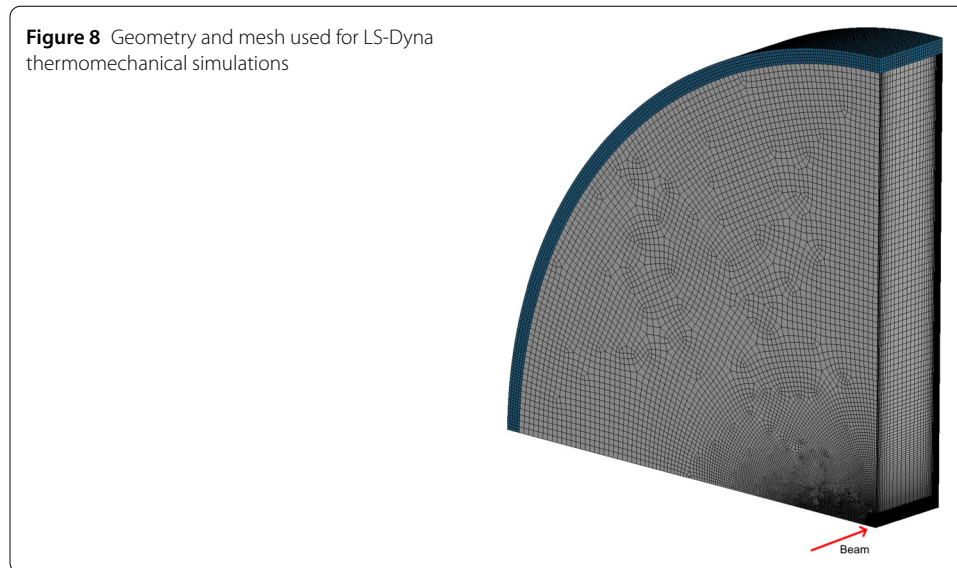
## 4 Simulation of the thermo-mechanical response

To simulate the thermo-mechanical response of the spoiler the finite element analysis software LS-Dyna [10] was used. The explicit mechanical solver was used in a tight coupled configuration together with a diagonal scaled conjugate gradient iterative solver for the transient thermal part of the simulation. A tight coupling of the thermal and mechanical solver ensures that dynamic effects within the material are simulated. The energy deposition results from the FLUKA simulation were imported as a heat generation source with a time dependent loading curve to match an overall FCC-ee beam pulse length of 168 μs.[1] This short pulse length was chosen as a conservative approach to highlight any possible dynamic effects. Since the main focus was on the immediate material response and not on long term effects, the time frame of interest is from the beam impact up to 1 ms. During this time the heat transfer between the surrounding environment and the spoiler is negligible. To further decrease the complexity and therefore the required computational time, the symmetry in the geometry as well as in the energy deposition was utilized. The simulation geometry was reduced to a quarter cylinder of the spoiler and symmetry boundary conditions were set accordingly (see Fig. 8).

For a tight coupled simulation in LS-Dyna two material models are needed for every component. To model the isostatic graphite material of the spoiler, a combination of an elastic mechanical model and a thermal isotropic model was chosen, including temperature dependent coefficients for density, thermal expansion and the elastic modulus as well as the specific heat and thermal conductivity.
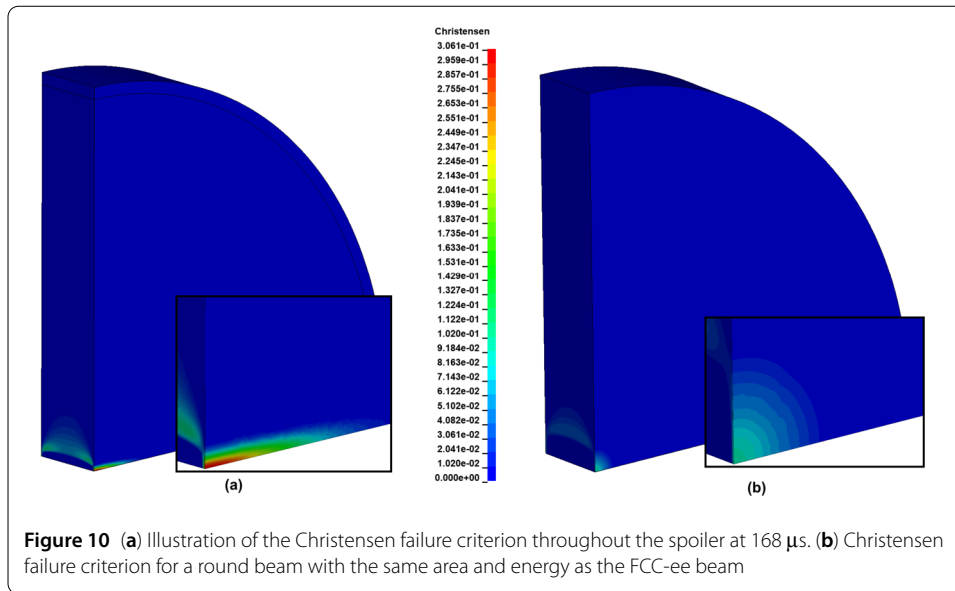
4.1 Material failure results

Due to the strong surface stresses and out of plane deformation induced by the beam impact, the most critical phase for the spoiler is at the end of the beam pulse. To evaluate the material response and whether the spoiler material is failing after beam impact, the Christensen failure criterion was used. Compared to other failure criteria (e.g. the von-Mises stress) the Christensen criterion is better suited to accurately describe brittle

---

[1]Assuming 10 ns bunch spacing (4th bucket fill) and no gaps between bunch trains.

Figure 9 (**a**) Peak value of the Christensen failure criterion over time. (**b**) largest principal stress value over time
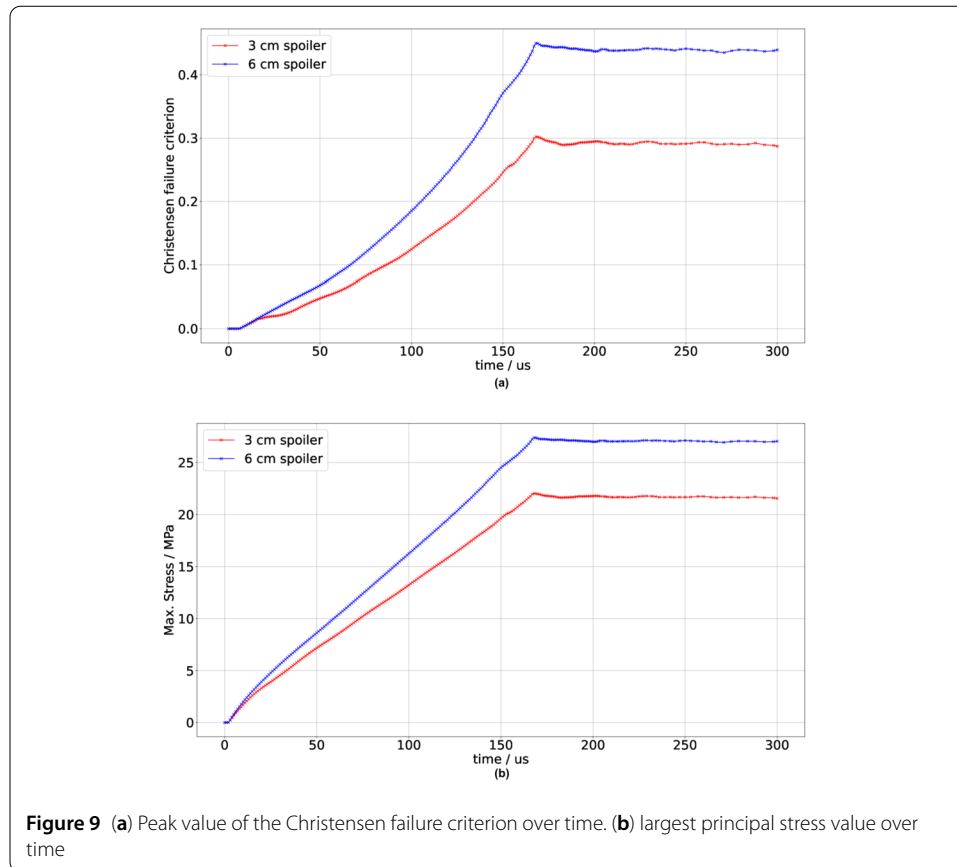
materials and especially materials in the intermediate range between ductile and brittle $(0 \leq \frac{\text{tensile strength}}{\text{compressive strength}} \leq 1)$ [11]. For an isotropic material the criterion describes a relation between the principal stresses (σ_{1-3}) and the maximum compressive and tensile strength of the material. For a material not to fail, the failure criterion value must be below 1 and all principal stresses must be smaller than the tensile strength limit. For the simulation, the values were taken to be 130 MPa for the compressive strength and 40 MPa for the tensile strength, which are the average properties of graphite grade R7550, produced by SGL [12]. Graphite also experiences strengthening with increasing temperature, which gives a safety margin when assuming the aforementioned values over the full temperature range. Figure 9 shows the evolution of the Christensen failure criterion value over time, as well as the largest principal stress for both the 3 cm spoiler and the 6 cm spoiler.

As can be seen, the failure criterion value always stays below 1, with a safety margin of a factor 3 for the 3 cm spoiler. Similarly, the largest principal stress is less than 40 MPa at all times. In Fig. 10(a) the failure criterion throughout the 3 cm spoiler can be seen at the time where the highest value occurs ($t = 168$ µs). The flat beam shape is clearly visible within the failure criterion distribution. Comparing this to the peak failure criterion value for a round electron beam with the same beam energy and area as the FCC-ee beam (see Fig. 10(b)), the influence of the transversal beam shape on the surface stress distribution and the likelihood of material failure is evident.

Figure 10 (**a**) Illustration of the Christensen failure criterion throughout the spoiler at 168 μs. (**b**) Christensen failure criterion for a round beam with the same area and energy as the FCC-ee beam

5 Conclusion

The FCC-ee is designed to be the highest intensity lepton collider. The nominal stored beam energy is 100 times higher than in any current or previous lepton storage rings. To ensure highest availability and improved safety, a semi-passive beam dilution system has been presented. The challenges in reliably extracting the beam from the main ring and increasing the beam spot size to a level where the spoilers can survive have been addressed and an extraction system has been designed which provides enough separation from the main ring to accommodate the beam dump and shielding. The performance of the spoilers has been assessed using Monte Carlo shower simulations, showing that the proposed dilution system is capable of diluting the beam enough to safely deposit it in the beam dump absorber. Furthermore, the thermo-mechanical response of the spoiler has been studied for different spoiler thicknesses showing that a three 3 cm spoiler system provides the best dilution as well as providing a safety factor of 3 against material failure.

Declarations

Competing interests
The authors declare that they have no competing interests.

Authors' contributions
WB initiated and revised the studies reading the beam extraction system described in Sect. 2. MC helped with the initial concept. YD contributed to the conception and revision of the beam extraction system. AL contributed to the initial conception of the dump system, created the initial Monte Carlo energy deposition studies and contributed to the improvement of said simulations as well as the result interpretation. APM gave major contribution to both, the

conceptualization as well as the setup for the thermo-mechanical studies and the interpretation of the results. SO created the initial extraction concept on which the current design is based. RR improved the initial beam extraction concept and created the current extraction system as well as the beam optics calculations, and was a major contributor in writing the manuscript. All authors read and approved the final manuscript.

Publisher's Note

References
1. Benedikt M et al. Future circular collider study. Volume 2: the lepton collider (FCC-ee) conceptual design report. Eur Phys J Spec Top. 2019;228(2):261–623. https://doi.org/10.1140/epjst/e2019-900045-4.
2. Akai K, Furukawa K, Koiso H. Superkekb collider. Nucl Instrum Methods Phys Res, Sect A, Accel Spectrom Detect Assoc Equip. 2018;907:188–99. https://doi.org/10.1016/j.nima.2018.08.017. Advances in Instrumentation and Experimental Methods (Special Issue in Honour of Kai Siegbahn).
3. Carlier E, Jansson U, Jung R, Mertens V, Péraire S, Ross M, Schröder G, Stevenson GR, Vossenberg EB, Weisse E, Zazula JM. The LEP beam dumping system, 4. 1994.
4. Maestre J, Torregrosa C, Kershaw K, Bracco C, Coiffet T, Ferrari M, Ximenes RF, Gilardoni S, Grenier D, Lechner A, Maire V, Ruiz JMM, Matheson E, Solieri N, Perillo-Marcone A, Polzin T, Rizzoglio V, Senajova D, Sharp C, Timmins M, Calviani M. Design and behaviour of the large hadron collider external beam dumps capable of receiving 539 MJ/dump. J Instrum. 2021;16(11):11019. https://doi.org/10.1088/1748-0221/16/11/p11019.
5. Goddard B, Gyr M, Uythoven JA, Veness R, Weterings W. LHC beam dumping system: extraction channel layout and acceptance. Conf Proc C. 2003;030512:1646.
6. Battistoni G, Böhlen T, Cerutti F, Chin PW, Esposito LS, Fassò A, Ferrari A, Lechner A, Empl A, Mairani A, Mereghetti A, Ortega PG, Ranft J, Roesler S, Sala PR, Vlachoudis V, Smirnov G. Overview of the FLUKA code. Ann Nucl Energy. 2015;82:10–8. https://doi.org/10.1016/j.anucene.2014.11.007.
7. Böhlen TT, Cerutti F, Chin MPW, Fassò A, Ferrari A, Ortega PG, Mairani A, Sala PR, Smirnov G, Vlachoudis V. The fluka code: developments and challenges for high energy and medical applications. Nucl Data Sheets. 2014;120:211–4. https://doi.org/10.1016/j.nds.2014.07.049.
8. Ahdida C, Bozzato D, Calzolari D, Cerutti F, Charitonidis N, Cimmino A, Coronetti A, D'Alessandro GL, Donadon Servelle A, Esposito LS, Froeschl R, García Alía R, Gerbershagen A, Gilardoni S, Horváth D, Hugo G, Infantino A, Kouskoura V, Lechner A, Lefebvre B, Lerner G, Magistris M, Manousos A, Moryc G, Ogallar Ruiz F, Pozzi F, Prelipcean D, Roesler S, Rossi R, Sabaté Gilarte M, Salvat Pujol F, Schoofs P, Stránský V, Theis C, Tsinganis A, Versaci R, Vlachoudis V, Waets A, Widorski M. New capabilities of the FLUKA multi-purpose code. Front Phys. 2022;9:788253. https://doi.org/10.3389/fphy.2021.788253.
9. FLUKA Website. 2021. https://fluka.cern. Accessed 13 Dec 2021.
10. LS-Dyna Website. 2021. https://www.lstc.com. Accessed 9 Dec 2021.
11. Christensen RM. The theory of materials failure. Oxford: Oxford University Press; 2013.
12. SIGRAFINE® R7550 Datasheet. https://www.sglcarbon.com/pdf/SGL-Datasheet-SIGRAFINE-R7550-EN.pdf. Accessed 17 Nov 2021.